ARC-ELECTRODE INTERACTIONS IN SILICON AND FERROSILICON FURNACES

G. Sævarsdottir[1], M.Th. Jonsson[1] and J.A.Bakken[2]

[1]Dept. of Mechanical Engineering, University of Iceland. E-mail: gudrunsa@hi.is, magnusj@hi.is
[2] Dept. of Materials Technology, Norwegian University of Science and Technology. E-mail: jabakken@nt.ntnu.no

ABSTRACT

A typical three-phase submerged-arc furnace for production of silicon metal and ferrosilicon has arc currents ~100 kA, phase voltages ~100 V and total furnace power ~10 - 60 MW. The arcs burn in gas filled cavities or "craters", where the main atomic components of the plasma mixture are silicon, oxygen and carbon. Two quite different simulation models for high-current AC arcs have been developed: the simple Channel Arc Model (CAM), and the more sophisticated Magneto-Fluid-Dynamic Model (MFD). These models have been described extensively and results reported at INFACON-8 and INFACON-9, respectively.

The coupling between the arcs and the AC power source is described by a complete three-phase Electric Circuit Model.

Recent numerical modelling studies of industrial AC arcs show that the boundary conditions at the cathode and anode are critical for the simulation results.

A novel Cathode/Anode Sub-Model for high-current AC arcs that treats both cathode and anode indicates a completely different cathode behaviour than previously assumed. A cathode spot which serves a high-current electric arc is shown to be dominated by the energy impact from the arc. This leads to lower cathode fall voltage than obtained from previously developed models. The anode fall voltage is negative, as the main function of the potential barrier is to repel plasma electrons. The cathode spot is diffuse in the sense that the arc in fact contracts away from the cathode.

Simulation results are compared to measurements on both industrial furnaces and smaller scale pilot furnaces. An important conclusion, supported by our arc studies, is that the arc length in silicon metal and ferrosilicon furnaces does not exceed 15 cm and the arc may burn anywhere on the electrode, not necessarily beneath the electrode tip.

1. INTRODUCTION

MFD simulation models for industrial AC arcs have been developed and published previously by the authors at the last INFACON-9 [1]. As arc behaviour is very sensitive to the boundary conditions at cathode and anode, considerable work has been put into the development of cathode sub-models for high-current AC arcs. In fact three generations of models have been developed. The first model, here called *the classic model* is based on the assumption that the cathode spot is self sustained with energy, and that the cathode fall voltage is constant all over the cathode spot, which in turn requires the cathode spot to deliver excess energy to the arc. The second model called *the variable u_C model* allows the cathode fall voltage to vary over the cathode spot, but assumes that an energy balance is fulfilled in each element of the cathode. The weakness of this model is that when energy transfer by radiation from the arc is taken into account, the integrated current density from the model is much higher than the total arc current. Therefore measures must be taken to reduce the total integrated current, and as a response a third model, specific for *high-current* arcs was developed. *The diffuse spot cathode / anode model*, is different from the first two in that it does not require the energy balance in the ionization layer to be fulfilled as there is an abundance of energy from the electric arc that enters this layer. The cathode fall voltage is assumed constant over the cathode surface and determined by the requirement that the total current from the electrode should be equal to the imposed arc current. The

anode is treated in the same formal way as the cathode. This model is the most promising of the three in the case of a high-current industrial arc, corresponding to the limit of an arc dominated cathode spot. Results from this model predict an arc attachment of a larger diameter than the arc itself, in addition to negative anode fall voltage.

2. GENERAL CATHODE SPOT THEORY

2.1 The plasma sheath

If there initially is a wide body of plasma at local thermodynamic equilibrium (LTE) and suddenly a part of it is surrounded by an isolating wall, the wall will initially be bombarded and charged up by fast moving plasma electrons. The negatively charged wall will then repel approaching plasma electrons and attract ions, thus forming a *space charge sheath* that shields the plasma gas from the effect of the negatively charged wall. Approaching plasma electrons will not notice the wall before they enter the space charge sheath, but as they penetrate the ion layer the shielding effect is reduced and they are slowed down by the electric field.

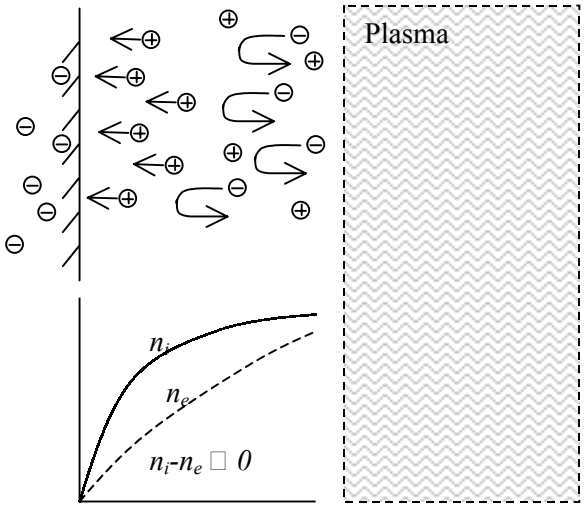

Figure 1. Schematic drawing of a space charge sheath.

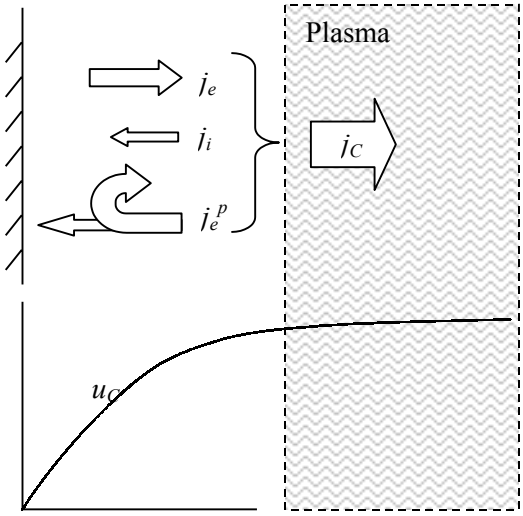

Figure 2. Current components in the cathode sub-models.

For an isolating wall the potential drop in the sheath is exactly high enough to ensure zero total current. When a net current is applied upon a plasma contained between two walls, it is natural to assume that the potential fall is adjusted such that the there is a net charge exchange between the plasma and the wall consistent with the applied current. The thickness of this space charge sheath is approximately $25\lambda_D$ which is close to 1 μm and orders of magnitude smaller than the thermal boundary layer, which in the case of an industrial arc is close to 500 μm.

2.2 General expressions

The AC cathode sub-models (CSM) to be described here are all based on the following assumptions: The cathode spot current density j is composed of three components: Thermionically emitted electrons j_e, ions from the plasma that reach the cathode surface j_i, and finally plasma electrons that pass through the potential barrier and reach the surface j_{epl} The models are to a certain extent based on ideas appearing in Neumann's theory [2] and Benilov's model [3] for low-current DC arc cathodes.

Neumann's theory is based on a simple energy balance for the ionization layer plus Richardson-Dushman's equation for the thermionic emission current density with the Schottky term given in Equations 1 and 2. The space charge and electric field distributions are not calculated, but the ion saturation current in Equation 5 gives an upper limit to the ion current. The heat flux q_C to the cathode is expressed as a function of the surface temperature T_C as seen in Equation 8 apart from the fact that radiative heat exchange is omitted. It is a simplified model which uses a stationary solution of Fourier's equation for a uniform heat source on a semi-infinite body.

Benilov's model gives an asymptotic solution of the "non-linear heat structure problem". The heat flux exhibits a peculiar behavior: At lower temperatures it increases with T_C to a maximum and then drops fast to 0. Benilov's model is asymptotic in the sense that the solution is obtained for the limiting case of a very narrow profile. Important results are that the cathode fall voltage u_C decreases with increasing arc current I, first very sharply and then slowly, approaching a minimum value for $I \to \infty$. The average current density j increases slowly with the current and the spot radius R_C increases therefore faster.

When a body is sufficiently hot, a fraction of its electrons have kinetic energy high enough for them to overcome the energy barrier called the work function ϕ which traps them in the body. The thermionic emission current density is given by Richardson-Dushman's equation :

$$j_e(T_C) = 1.2 \cdot 10^6 T_C^{\,2} f \exp\left(\frac{e(\ddot{o} + \ddot{A}\ddot{o})}{k_B T_C}\right) \tag{1}$$

where: T_C denotes the cathode surface temperature, e is the electronic charge, ϕ is the thermionic work function, k_B is Boltzmann's constant and Δϕ is the Schottky correction as used in these simulations:

$$\begin{aligned} \ddot{A}\ddot{o} &= \sqrt{\frac{eE_C}{4\eth\aa_0}} \\ E_C^2 &= \frac{4 j_i}{\aa_0}\sqrt{\frac{m_i u_C}{2e}}\left(\sqrt{1+\frac{T_e}{7993.0\,u_C}} - 1.34443\sqrt{\frac{T_e}{7.993.0\,u_C}}\right) \end{aligned} \tag{2}$$

where: m_e the electron mass, m_i the ion mass, h is Planck's constant and finally ε_0 is the electric permittivity of vacuum. The Schottky correction term Δϕ reduces ϕ for carbon from the assumed 4.75 eV by 0.5 eV or less. The expression for E_C is known as MacKeown´s equation. In general, the Schottky term did not have a significant influence on the results. The factor f in the Richardson Dushman equation is a scaling factor accounting for the fact that a thermionically emitted current with the theoretical value of $f = 1$ has never been observed. According to Pfender et al.'s [4] estimate $f = 0.5$, which is used in this work.

The hot plasma gas contributes electrons that are energetic enough to climb the cathode fall potential u_C and enter the cathode. *The counter-diffusing plasma electron current* is given by:

$$\begin{aligned} j_{epl} &= \frac{1}{4} e n_{e0} c_e e^{-eu_c / k_B T_c} \\ c_e &= \sqrt{\frac{8 k_B T_e}{m_e \pi}} \end{aligned} \tag{3}$$

where: n_{e0} is the electron density at the edge of the space charge sheath, and c_e is the mean electron velocity in each direction

The ion current [5] [6] towards the cathode is given by the Bohm velocity v_B :

$$\begin{aligned} j_i &= e n_{i\infty} v_s f_w \\ v_s \geq v_B &= \sqrt{\frac{k_B T_e}{m_i}} \end{aligned} \tag{4}$$

$n_{i\infty}$ is the ion density at the edge of the ionization layer where the gas is close to full ionization. f_w represents the relative ion density $n_{i0}/n_{i\infty}$ at the sheath edge. In Equation 3 n_{e0}, which equals n_{i0}, could then be expressed as $n_{i\infty} f_w$. Benilov *et al* [3] reported equations for f_w and v_s that lead to the following expression for the ion current density:

$$j_{isat} = n_{i\infty} \frac{0.8}{2+\alpha} \sqrt{\frac{k_B(T_C + T_e)}{M_i}}$$
$$\alpha = \sqrt{\frac{k_B T_h}{m_i D_{ia\infty} k_r n_{i\infty}^2}} \qquad (5)$$

where: D_{ia} is the ion-atom diffusion coefficient, k_r is the ion-electron recombination rate coefficient and T_h the heavy particle temperature, all evaluated at the edge of the ionization layer. The important parameter α is associated with the ratio of the thickness d of the ionization layer to the mean free path for ion-atom collisions λ_{ia}. The fraction $0.8/(2+\alpha)$ in Equation 5 reaches its maximum of 0.4 as α approaches 0. In this case $\alpha=10^{-3}$. The term ion *saturation* current indicates that the ion current is not allowed to rise above this value, but can be lower. This is how the equation is used in *the classic model*. In *the variable u_C cathode sub-model*, however, the ion current density j_i is set equal to j_{isat} in Equation 5. If it is assumed that the energy balance for the ionization of atoms by emitted electrons is fulfilled in the ionization layer all over the cathode spot, the radially dependent cathode fall voltage $u_C(r)$ can be determined:

$$j_e\left(u_C + 2\frac{k_B T_C}{e} - 3.2\frac{k_B T_e}{e}\right) = j_i\left(U_i + 2\frac{k_B T_i}{e} + 3.2\frac{k_B T_e}{e} - 2\frac{k_B T_C}{e}\right)$$
$$+ j_{epl}\left(u_C - 1.2\frac{k_B T_e}{e}\right) \qquad (6)$$

Here j_e and j_i represent the electron and ion current densities in the near cathode layer and U_i is the ionization potential. The thermionically emitted electrons are accelerated over the space charge sheath potential fall u_D, In the model presented by Benilov *et al*. u_D is the voltage drop in the space charge sheath, and u_i is the voltage drop in the ionization layer. The cathode fall voltage is the sum of these two contributions: $u_C = u_D + u_i$. As in general $u_i/u_D << 1$ and it is only possible to determine one independent parameter in this model, we assume that $u_i = 0$ and $u_C = u_D$. The thermionic electrons are emitted with their two-dimensional enthalpy in equilibrium with the cathode body, but need to be heated up to the plasma temperature to be in thermodynamic equilibrium. The energy supplied by the thermionic electrons is used to ionize atoms, and bring the electrons displaced from the atoms to equilibrium with the arc plasma. The counter-diffusing electrons must overcome the space charge potential, and carry a two-dimensional enthalpy to the cathode.

In addition comes the j_{epl} part of the kinetic energy carried by the total current density towards the bulk plasma $j*3.2(k_B T_e/e)$. The energy balance is based on enthalpy, so the factor is 5/2 instead of 3/2 for the kinetic energy. The factor 2 instead of 5/2 in front of $k_B T_C/e$ in equilibrium with the cathode is caused by the loss of one dimension assuming that the kinetic energy perpendicular to the cathode is used up climbing the cathode fall potential. Accordingly the factor 3.2 for the kinetic energy in equilibrium with the arc plasma, is composed of 5/2 accounting for enthalpy transport due to the electric current and of a thermal diffusion coefficient $0.7(k_B T_e/e)$ calculated for a strongly ionized plasma. T_e and T_i are the electron and ion temperatures, that are equal under LTE conditions. At the edge of the ionization layer, however, it is more correct to put $T_i = T_c$.

An extension to AC is accomplished by imposing a periodically varying arc current. The non-steady two-dimensional axi-symmetric Fourier equation is solved for the electrode body using the heat flux in Equation 7 as a boundary condition, to obtain a periodically varying cathode surface temperature $T_c(r,t)$. The computational domain is assumed large compared to the cathode spot radius (0.1 m) in the radial direction and to the thermal penetration depth of 50 Hz temperature oscillations (1 mm) in the axial direction.

The cathode heat flux assumes the following form:

$$\dot{q}_c = j_i(u_c + 2\frac{k_B T_i}{e} - 2\frac{k_B T_C}{e} + U_i - \phi) - j_e\left(2\frac{k_B T_C}{e} + \phi\right) + j_{epl}\left(2\frac{k_B T_e}{e} + \phi\right) + \dot{s}_{rad} \quad (7)$$

Radiation from the arc as well as energy contributed by the particle impact on the surface during the anodic half-period is considered, and calculated values from the MFD model are used. However, ohmic heating in the electrode is disregarded as it is judged as insignificant as compared to the heat input from the arc and the particle impact in the cathode spot. The electromagnetic equations are not solved for the electrode body, and the current density within the electrode is not known. In the present results sublimation of the electrode body has not been taken into account, but the introduction of a *maximum temperature* ensures that the sublimation temperature is not surpassed.

3. MODEL I: THE CLASSIC CATHODE SUB-MODEL

The first generation of cathode model is included here as only preliminary results from it were published previously [1]:

- From the cathode temperature $T_c(r.t)$ the thermionic current density $j_e(r.t)$ is calculated from Richardson-Dushman's Equation 1
- The total arc current is integrated over the cathode surface.
- The cathode fall voltage $u_c(t)$ is assumed to be constant over the cathode surface and is determined from an energy balance modified from Equation 6 by removing the term for counter-diffusing plasma electrons:

$$j_e\left(u_c + 2\frac{k_B T_C}{e} - 3.2\frac{k_B T_e}{e}\right) = j_i\left(U_i + 2\frac{k_B T_i}{e} + 3.2\frac{k_B T_e}{e} - 2\frac{k_B T_C}{e} - u_c\right)$$

Here it is assumed that $T_i = T_e$.

- An equation for the heat flux is modified from Equation 7 by omitting the current of plasma electrons:

$$\dot{q}_c = j_i(u_c + 2\frac{k_B T_i}{e} - 2\frac{k_B T_C}{e} + U_i - \phi) - j_e\left(2\frac{k_B T_C}{e} + \phi\right) + \dot{s}_{rad}$$

Results where radiation is omitted, as has been the standard assumption in previous DC cathode models, as well as the previously published version of this model, are compared to calculations including radiation. The heat flux is then used as a boundary condition for the Fourier equation for the electrode body. The temperature at the cathode surface is then used in step 1. The heat flux to the cathode during the negative - i.e. anodic - half-period is neglected.

3.1 Results

The results presented for *the classic model* are for a model identical to the ones published previously [1] except for the fact that temperature and current distributions in the plasma at the cathode as well as radiation flux data are delivered by the MFD arc model. In [1] the temperature distribution in the plasma at the wall was assumed and arc radiation was ignored.

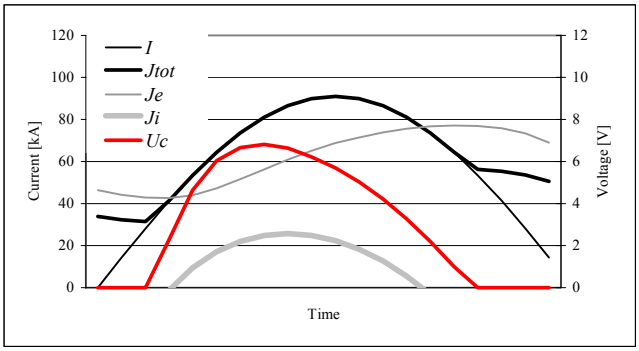

Figure 3. Total current and current components as well as the cathode fall voltage as calculated by the classic cathode sub-model including arc radiation. Note that close to passing through zero, the model does not give a solution - *Jtot* is larger than the arc current *I*.

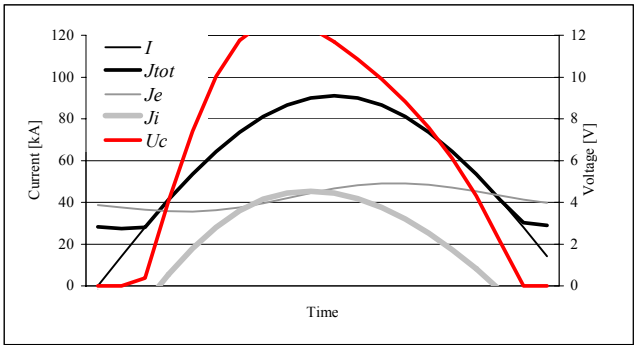

Figure 4.The same as except that arc radiation is *not* included in the heat flux to the cathode.

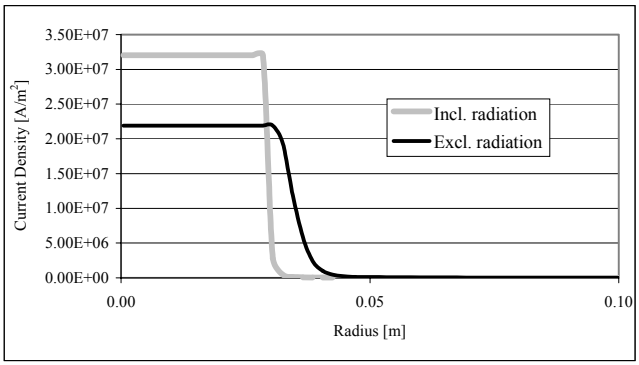

Figure 5. Current density as a function of radius at current maximum predicted by the classic cathode sub-model with and without radiation.

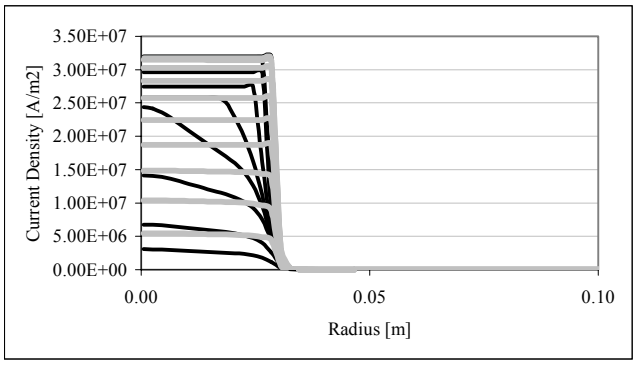

Figure 6. Current density as a function of radius in the cathode spot as calculated by the classic cathode sub-model, taking into account radiation from the arc. The black curves refer to the first quarter period while the current is rising and the grey curves to the second quarter period while the current is falling.

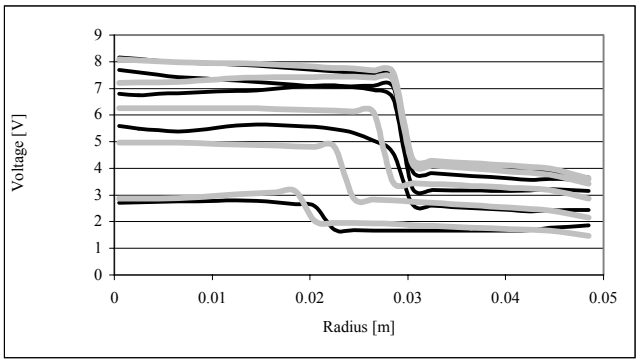

Figure 7. Variable U_c model: Cathode fall voltage as a function of radius at different instances of time during the half-period. Black lines represent rising and grey lines falling current

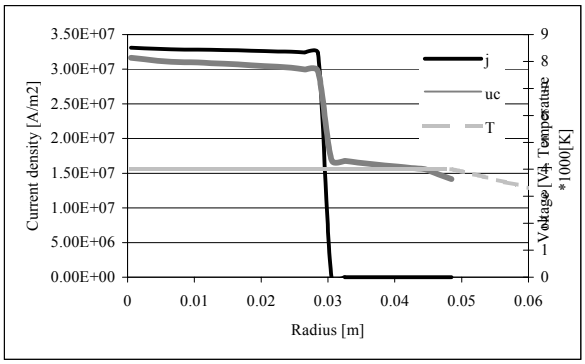

Figure 8. Variable U_c model: Different current density components as well as u_C and temperature shown as functions of radius at peak current.

In the previously published model the scaling factor f in Equation 1 is equal to the theoretical value 1, while in this work f is set to the empirical value 0.5. This will inevitably decrease the cathode current density. The cathode fall voltage u_C is calculated in the colder outskirts of the arc. This is because the usage of a constant cathode fall voltage, combined with the energy balance, leads to a higher j_i than the saturation current. As the ion current j_i cannot exceed the saturation current obtained from the cathode fall voltage, not all energy provided by the electrons accelerated through the cathode fall voltage is used for ionization of the atoms that deliver the ion current. Therefore the cathode fall voltage delivers an *excess* of energy to the ionization layer, and the energy balance is not fulfilled, for that particular cell. As a cell becomes so hot that the energy balance is no longer fulfilled, the cell is dropped in the cathode fall voltage calculation. The cathode fall voltage is calculated from the relatively colder cells of the cathode spot, where the energy balance is fulfilled. Figures 3 and 4 show the imposed arc current, the two current components J_e and J_i, and their sum J_{tot}, as well as the cathode fall voltage u_C. Figure 3 differs from Figure 4 in that radiation from the arc is included and contributes significantly to the heating up of the cathode. It can be seen that close to current zero, the total current calculated by the model J_{tot} exceeds the imposed arc current I. This means that no positive u_C leads to a solution. Figure 5 displays the current density in the cathode spot as a function of distance from the axis of symmetry shown for both cases. The current density distribution is relatively flat within the cathode spot and falls fast to zero outside the spot. Including radiation, a maximum current density of $3.2 \cdot 10^7 \mathrm{A/m^2}$ is obtained, while the current density is $2.2 \cdot 10^7 \mathrm{A/m^2}$ when radiation is ignored. This current density so large that used as a boundary condition in electric arc models it leads to a unreasonably high arc resistance, but nevertheless lower then the current density predicted by other models that in fact have been proposed for low-current DC arcs [7][8]. In Figure 6 current density as a function of radius is shown at intervals during the cathodic half-period. It can be seen that the cathode spot radius remains constant all through the half-period, while the current density is variable.

Three factors should be considered:

- The current of counter-diffusing plasma electrons that climb over the cathode fall potential and enter the cathode, must be taken into account.
- The excess energy delivered by the thermionically emitted electrons that have been accelerated through the cathode fall voltage, must be eliminated.
- The enormous amount of radiative energy delivered by the arc may not be neglected - cfr. Figures 3 and 4.

4. MODEL II: THE VARIABLE UC SUB-MODEL

The most significant limitation of *the classic cathode sub-model* is the omission of plasma electrons. Another important physical limitation in the classic model is the fact that the energy balance is not fulfilled over most of the cathode spot. It is quite unphysical that the ionization layer of a cathode that serves an intense high-current industrial arc, delivers energy to the arc, but does not receive any. Another model - *the variable u_C cathode sub-model* - was therefore developed to take these factors into consideration. The most important changes from the classic model are that *the cathode fall voltage u_C is allowed to vary over the cathode surface* to ensure that the energy balance is fulfilled in each cell, and that the counter-diffusing plasma electrons j_{epl}, that climb the cathode fall potential and diffuse back towards the cathode, are taken into account in the new model II. This current is given in Equation 3. In addition, the ion current $j_i(r)$ is assumed to be equal to the ion saturation current as defined in Equation 5 and. The main assumption is therefore that the energy balance in Equation 6 is valid in each cell of the cathode spot. The energy flux from the arc by radiation and particle impact keeps the cathode surface temperature so high that the area of the cathode that emits electrons is much larger then that needed for the integrated current to be equal to the imposed arc current. The problem is therefore how to ensure that the integrated current is equal to the arc current. This was done by limiting the size of the cathode spot by restricting the integration to only those cells that are needed to deliver the imposed arc current. The voltage in the cells outside is calculated such that the current density is equal to zero. This is of course not a satisfactory method to limit the current, but if data delivered by the arc model is to be used such measures must be taken. This will be further commented upon at the end of this section.

4.1 Results

The total cathode spot current is composed of three large components, thermionically emitted electrons, the ion current from the plasma and the counter-diffusing plasma electrons The total current is then the sum of these components. These current components are calculated by the variable u_C CSM as functions of time during the cathode half-period. J_e and J_{epl} are each larger then the total current. The current density over the cathode surface plotted at regular intervals during the cathode half-period is shown in Figure 8, and in Figure 7, u_C is shown as a function of radius. It is interesting to see that the current density and cathode fall voltage is relatively flat over the active cathode spot, but the level is time dependent, as well as the cathode spot radius. The variable cathode spot radius is without doubt a result of the restraint on the cathode spot radius made by the imposed arc current. The variable cathode fall voltage can easily be taken into account in the MFD arc model by locally adjusting the electric conductivity. As previously pointed out, this method to limit the current is not satisfactory, and for a correct model with correct boundary conditions, the total integrated current should equal the arc current without such measures. The main uncertainty here is the temperature of the plasma gas at the cathode surface. Should it be justified to apply the energy balance in Equation 6 and the heat flux in Equation 7, a correct temperature profile in the plasma is crucial. Therefore an overall energy balance for the cathode / anode - arc system should be fulfilled. All this inspired the development of the so called *diffuse spot cathode / anode sub-model*.

5. THE DIFFUSE SPOT CATHODE/ANODE SUB-MODEL

The diffuse spot cathode/anode sub-model (CASM) to be described here is based on the fact that in a relatively short high-current industrial arc, the energy supply from the arc is so overwhelming that it is not possible to divide the cathode and the arc into two separate energy domains that do not exchange energy. For the energy balance in Equation 6 to be fulfilled, the temperature of the plasma at the cathode surface must be correct. It cannot be required that thermionically emitted electrons accelerated through the cathode fall supply all energy required to sustain the arc spot as the radiation from the arc and the abundance of much more energetic plasma electrons is sufficient to ionize neutral atoms and equilibrate colder electrons. This means that instead of *two separate energy balances*, Equation 7 on the one side, and the MFD transport equations for the arc on the other, an energy balance for the whole system must be solved *within the MFD model.* In the CASM only the energy balance for the electrode itself, using boundary conditions in Eq. 7 will be considered. The heat flux into the cathode/anode body must be used as a boundary condition for the arc model. In this new model cathode and anode are considered to be formally identical, and the total current balance

$$I(t) = 2\pi \int_0^{r_{\max}} j_e(r,t) r dr + 2\pi \int_0^{r_{\max}} j_{isat}(r,t) r dr - 2\pi \int_0^{r_{\max}} j_{epl}(r,t) r dr \qquad (8)$$

is fulfilled at any time for both electrodes. This means that the cathode as well as the anode thermionically emit electrons consistent with their temperatures, and that they are both bombarded with plasma electrons and ions dependent on the temperature of the plasma next to the electrode. The difference between cathode and anode is only that the net current is negative in the cathodic half-period and positive in the anodic half-period. The cathode/anode fall voltage, here termed u_C for consistency, is determined by solving Equation 8 for the given current at each timestep. Radiation fluxes and plasma temperatures are obtained from arc simulations. For this model to be correct it will be necessary to couple the MFD arc model and the cathode /anode sub-model and solve both models simultaneously. This has not been possible within the time frame of this work, but a tentative iterative procedure is used.

5.1 Model description

When a net current is applied upon a plasma contained between two walls, it is natural to assume that the potential fall is adjusted such that the there is a net charge exchange between the plasma and the wall consistent with the applied current. In the simulations it is assumed that the cathode/anode body is a good current conductor as compared to plasma. The electrical conductivity of a typical electrode mass at high temperatures is of the order $\sigma \approx 5 \cdot 10^4$ - $1 \cdot 10^5$ S/m, whereas $\sigma \approx 5 \cdot 10^3$ - $1 \cdot 10^4$ S/m for the plasma close to the electrode. This means that the assumption that the electrodes are perfect conductors is not quite accurate. Anyway, in the time frame of the work reported here a model that solves the transport equation for the magnetic field within the electrode body has not yet been developed, but this would be necessary to

determine the current distribution within the electrode. Therefore this simplifying assumption had to be made.

Although the electrode is considered as a perfect conductor that does not imply that the electrode necessarily has a uniform potential over its surface. As the tangential component of an electric field is always continuous over a surface, the electric field must be normal to the surface. Therefore the surface charge will arrange itself with regard to the space charge in the sheath in such a manner that this criterion is fulfilled. Nevertheless we assume in this model that u_C is constant over the surface.

As already mentioned, the current density at the cathode is composed of three different components: the thermionically emitted current, the current of plasma electrons towards the cathode in Equation 3, and finally the ion current. As previously pointed out, the abundance of energy provided by the electric arc is such that the energy balance in Equation 8 is not fulfilled, separated from the arc. The anode/cathode surface thermionically emits electrons in accordance with its temperature (and with a weak dependence on the potential fall). It receives ions from the plasma, and the potential fall regulates the influx of plasma electrons such that Equation 7 is fulfilled.

But as the heat flux by particle impact in Equation 7 includes heat transport due to ambipolar diffusion and heat flux due to current, the boundary condition for heat transport in plasma must be set up correspondingly. Here it has been assumed that convective/conductive heat transport is negligible in comparison. Data for the thermal conductivity (and other transport coefficients) for two-temperature Si-O-C plasmas, is not yet available. However, heat transport due to ambipolar diffusion is probably the most important contributor.

The heat flux to the wall as well as the power generated by the electrons accelerated in the potential, must be included as a source (or sink) term in the MFD arc model. The source term to be included in the cells next to the cathode/anode surfaces has the form:

$$\dot{q}_{bound} = -j_i\left(2\frac{k_B T_i}{e} - 2\frac{k_B T_C}{e} + U_i\right) + j_e\left(u_C + 2\frac{k_B T_C}{e}\right) - j_{epl}\left(u_C + 2\frac{k_B T_e}{e}\right) \qquad (9)$$

Notice that the thermionic work function ϕ terms have been removed as ϕ is exclusively a material property, which determines the energy of an electron within the material as compared to a free electron. The electric arc is not directly affected by the work function except by the work function's effect on the current density of emitted electrons. The same equations apply at the anode.

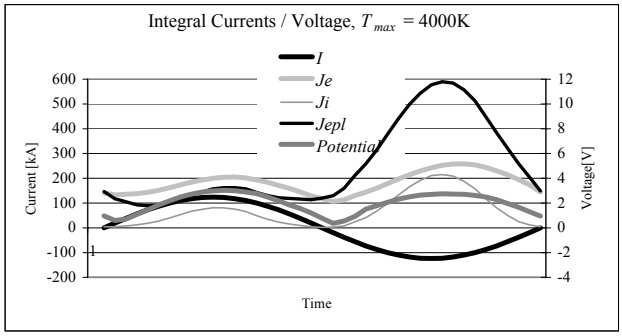

Figure 9. Integral current components and cathode/ anode fall voltages. The first half period is the cathodic and the second is the anodic half-period. The maximum material temperature is 4000 K.

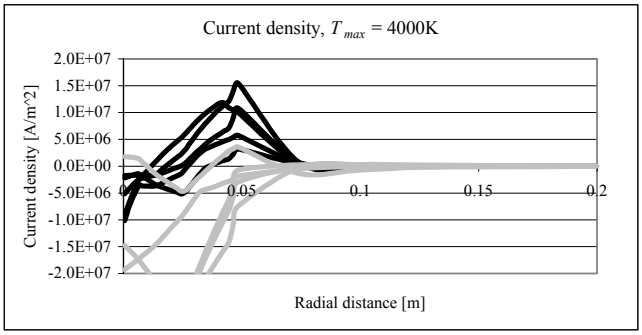

Figure 10. Current distributions for T_{max}= 4000 K at even time intervals through an AC period. The black curves refer to the cathodic half-period and the grey curves to the anodic half-period.

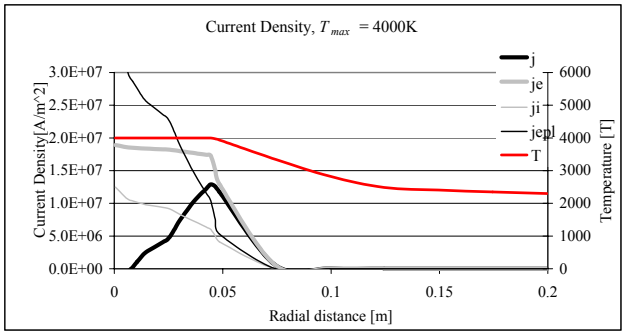

Figure 11. The current density distributions of the three current components at peak current in the cathode half-period as well as the resulting total current density and the cathode temperature profile. T_{max}= 4000K.

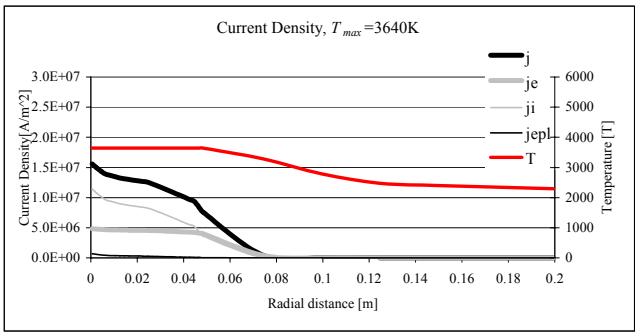

Figure 12. Same as Figure 11 in the case of T_{max}= 3640 K.

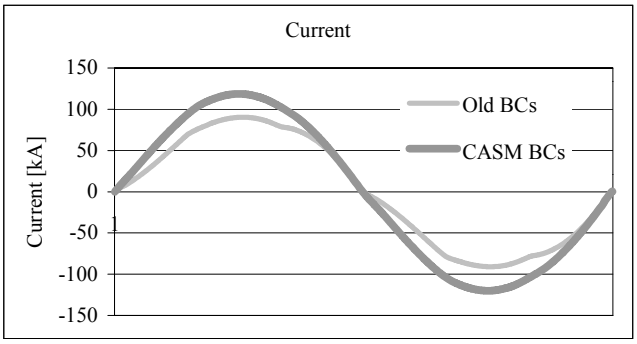

Figure 13. Current waveforms calculated for a 5 cm long industrial arc with the old type of boundary conditions as compared to CASM boundary conditions, for both single phase and three phase simulations.

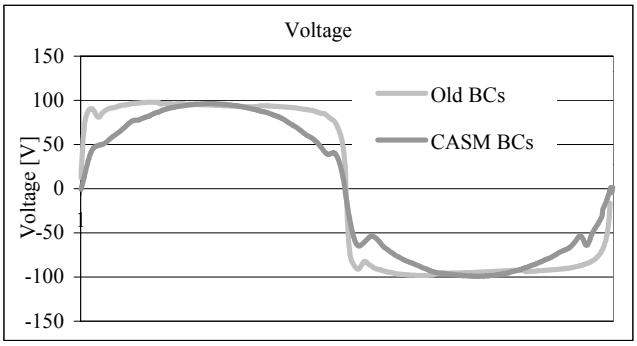

Figure 14. Voltage waveforms corresponding to the current waveforms in Figure 9.

Table 1. The maximum values of the various current densities [A/m^2] components at two electrode material temperatures. The cathode fall voltage [V] is shown as well.

Max. cathode temperature	**4000 K**	**3640 K**
u_c	2.9	5.8
j (r = 0)	-1.00·10^7	1.50·10^7
j_e (r = 0)	1.90·10^7	0.50·10^7
j_{epl} (r = 0)	3.98·10^7	0.05·10^7
J_i(r = 0)	1.08·10^7	1.07·10^7

5.2 Simulation results

When the energy balance is omitted and the potential drop u_C is assumed constant, u_C decreases, and thereby the plasma electron current density j_{epl} increases exponentially. This leads to a much lower total current density in the cathode (anode) spot dependent on the plasma temperature. If the plasma temperature is high enough, that results in a negative current density in a part of the arc spot. The resulting total current is composed of three components, two of which have a much higher total value than their difference. Figure 9 displays the time variation in the total current and the integral current components as well as the cathode and anodic fall voltages for maximum cathode temperatures 4000 K. It is seen that the three current components are each larger, and in the anodic half-period much larger, than the resulting total current. Another result is that the potential fall required to hamper the flow of plasma electrons in the anodic half-period is only about 0.3 V lower than the cathode fall voltage in the case of the 'hot' electrode. In the cathodic half-period the voltage reaches a maximum at 3.0 V and in the anodic half-period the maximum voltage is 2.7 V.

All this only demonstrates the necessity of coupling together the MFD arc model and the cathode / anode model to get more reliable values for the plasma temperature at the surface. It should be kept in mind that between the two half periods the overall arc voltage has changed sign, so that the anode fall voltage is indeed *subtracted* from the arc voltage – we have a *negative* anode fall. Let us now consider the current distribution at the surface. The plasma temperature at the electrode varies with the distance from spot center. The potential fall is, however, constant over the surface, so inevitably, the current density distribution is strongly varying. Figure 10 shows the time-varying cathode current density as a function of radius with a maximum cathode temperature of 4000 K. It is seen that the current density is negative in the center of the arc spot both in the anodic and cathodic half-periods.

Figures 11 and 12 show the radial distributions of the current density components at peak current with a maximum cathode surface temperature of 4000 K and 3640 K, respectively. The cathode radial temperature distribution is shown as well. The most obvious difference between the two sets of current densities is that all densities are lower for the colder cathode. Lower cathode surface temperatures naturally lead to lower thermionic emission of electrons j_e, and therefor a higher cathode fall voltage is needed to hamper the flow of plasma electrons towards the cathode surface. The cathode fall voltage is thereby increased from 2.9 V up to 5.8 V. The plasma electron current density j_{epl} is insignificant for the colder cathode, and therefore the resulting current density is a rather smooth curve with its highest value at the cathode spot center. The hotter cathode emits thermionically a larger amount of electrons. Therefore it must receive more plasma electrons to keep the balance, and the voltage is half of that of the colder electrode. As a result, the total current density is negative at the center of the cathode spot, while it is positive over the main part of the cathode. Such a current density profile is rather unphysical and would probably not occur if the electromagnetic equations were solved for the electrode body, and the energy balance for the entire arc/cathode system were properly fulfilled. These results are summed up in Table 1.

5.3 Effect on industrial arc simulations

MFD simulations have been performed on the high-current AC arcs expected to exist in the craters of a 30 MVA three-phase submerged-arc furnace for production of *silicon metal*. The crater gas was assumed to consist of SiO and CO in molecular ratio 1:1 with or without Al and Ca contaminations. The computational domain again corresponds to the assumed shape and size of the crater cavity of the industrial furnace. The arc length was varied from 5 to 20 cm. It was soon found that arc lengths of 5 – 10 cm gave the best fit to industrial data. The available transformer secondary voltage is not high enough to sustain e.g. a 20 cm long arc. As an example, Figures 13 and 14 show the simulated current and voltage waveforms for a 5 cm long arc in pure SiO-CO gas. The results shown here are for three-phase calculations using both the traditional boundary conditions (Old BCs) with a constant parabolic cathode current density with a mean value of $j_c = 1.4 \cdot 10^7 \mathrm{A/m^2}$ and the new BCs obtained by the cathode / anode sub - model (CASM).

The voltage waveform resembles a square wave. Neglecting parallel charge conduction, the calculated RMS currents for a 5 cm long arc varies from 64.5 kA using the older type of boundary conditions, up to 84 kA with the boundary conditions based on the CASM. A normal RMS electrode current for the furnace in question is around 80 kA, and the measured voltage between electrode holder and furnace bottom 100 V. That corresponds to approximately 80 V over the arc, when phase resistance and inductance have been accounted for. In an industrial furnace under normal operation it is generally believed that a part of the electrode current bypasses the arc and goes through the charge material surrounding the electrode. That will lead to a larger electrode current, at the same transformer voltage, than shown here for the pure arc. The recent CASM boundary conditions that considerably reduce the arc resistance, actually allow a longer arc. Simulations of a 10 cm long arc using the recent boundary condition give a RMS current of 56 kA and a RMS voltage of 110 V. If a charge current is taken into account, realistic electrode currents and voltages are obtained.

Table 2. Results of MFD simulations of industrial arcs. The corresponding current and voltage waveforms are shown in Figures 13 and 14.

Data	Old BCs	CASM-BCs
I_{rms} [kA]	64.5	84.6
U_{rms} [V]	90.1	78.4
P [MW]	5.4	6.5

6. DISCUSSION AND CONCLUSIONS

Three cathode models have been developed and are discussed in this paper. The first is the most primitive one and the second one was developed in order to solve some of the problems encountered in the first one. The problems connected to limiting the current in the second model lead to the development of *the diffuse spot cathode/anode sub-model*. The diffuse spot model deviates in important aspects from cathode models that have been reported in the literature. Most existing models have been made for low-current DC arcs, where the cathode spot must be energetically self-sustained, and no energy is extracted from the arc itself. This novel model represents the other limit: The cathode/anode spot is dominated by energy impact from the arc, and must be included in the energy balance for the arc itself. Although the CASM has not yet been fully integrated into the MFD arc model, the tentative iterative results indicate a much lower cathode current density than previously assumed and a much smaller cathode fall voltage, which indeed has the same sign in the anodic half-period. This means that in the voltage considerations for the total arc-cathode-anode system, the voltages for the cathode and anode almost cancel out! A *negative* anode fall voltage has previously been suggested by Pfender [9], but the standard assumption is that cathode and anode fall voltages add up. The relatively low current density gives rise to a diffuse cathode spot, wider than the part of the arc attached to it. Such diffuse cathode spots have been observed and discussed in connection with electric arc furnaces for steelmaking.

This diffuse arc spot also leads to a smaller resistance in the arc itself. Changing the arc boundary conditions in this direction in fact allows us to lengthen the arc from 5 to 10 cm and maintain a reasonable phase resistance *neglecting the charge conduction*. Taking charge conduction into account, assuming that for example half of the electrode current passes through the charge [10], the arc resistance may be increased and the arc itself lengthened accordingly, but still the order of magnitude is the same. The arc length is not much more than 15 cm.

7. REFERENCES

[1] Sævarsdottir, G.A., Bakken, J.A., Sevastyanenko, V.G., Gu Liping, “Arc Simulation Model for Three-Phase

[2] Electro-Metallurgical Furnaces”, INFACON 9, June 2001, Quebec City, Canada. In proceedings pp.253-263.

[3] Neumann, W., “The mechanism of the thermoemitting arc cathode”, Akademi-Verlag, Berlin, 1987.

[4] Benilov, M.S. “ The ion flux from a thermal plasma to a surface”, J.Phys. D: Applied Phys. 28, 1995, pp.286-294.

[5] Pfender, E., Boulos, M., Fauchais, P., “Methods and Principles of Plasma Generation”, "Plasma Technology in Metallurgical Processes", pp. 27-47, ISS-1987.

[6] Liebenham, M.A, Lichtenber, A.J, “Principles of plasma discharges and materials processing”, 1994, John Wiley and Sons , NY.

[7] Benilov, M.S., Naidis, G.V., “Ionization layer at the edge of a fully ionized plasma”, Physical Review E, Vol 57, No 2, Feb 1998.

[8] Bötticher, R., Bötticher, W., “Numerical modelling of arc attachment to cathodes of high-intensity discharge lamps”, J.Phys D: Appl. Phys. 33 (2000) pp. 367-374.

[9] Kaddani, A., Zahrai, S., Simon, O., “Kinetic model for the space charge zone in the cathode region of electric arcs”, ABB Technical report SECRC/KB/TR-95/244E, Vesterås, Sweden, 1995.

[10] Sanders, N., Pfender, E., “Measurements of anode falls and anode heat transfer in atmospheric pressure high intensity arcs”, J. Appl. Phys. 55 (1984) pp. 4136-4145.

[11] Sævarsdottir, G.A., “High Current AC Arcs in Silicon and Ferrosilicon Furnaces”, Ph.D. thesis 2002:36, Norwegian University of Science and Technology, Trondheim, 2002.